J. Fluid Mech. (1992), *vol.* 242, *pp.* 371–386
Printed in Great Britain

Buoyancy effects in vertical shear dispersion

By RONALD SMITH
Department of Mathematical Sciences, University of Technology, Loughborough, LE11 3TU, UK

(Received 15 October 1991)

Density gradients modify the flow and hence the shear dispersion of one miscible fluid in another. A solution procedure is given for calculating the effects of weak buoyancy for vertical laminar parallel shear flows. A particular extrapolation to large buoyancy gives an exactly solvable nonlinear diffusion equation. For the particular case of vertical plane Poiseuille flow explicit formulae are derived for the flow, for the nonlinear shear dispersion coefficient and for the onset of instability. The exactly solvable model gives reasonably accurate results for the buoyancy-modified shear dispersion over a range from half to one-and-a-half times the non-buoyant value.

1. Introduction

Long (1991) describes a series of elegant laboratory experiments involving the upwards miscible displacement of a Newtonian fluid by a denser Newtonian fluid in a narrow vertical annulus. The purpose of his experiments was to quantify and to give detailed flow visualizations for some of the flow phenomena encountered in the final stages of drilling an oil well when the narrow region outside the steel casing is flushed clear of drilling fluid and then the cleaning fluid is in turn displaced from below by cement. A laboratory experiment of height 3 m cannot easily encompass the full range of flow conditions that can arise in a borehole of depth 6 km or even more. Fortunately, the opposite extreme when the zone of mixing has become very long, lends itself to mathematical analysis.

In one of the most cited papers in the entire subject of fluid mechanics, Taylor (1953) showed that the eventual evolution of dilute solute concentration in a flow is longitudinal and diffusive:

$$\partial_t \bar{c} + \bar{w}\,\partial_z \bar{c} - [\bar{\kappa} + D_0]\,\partial_z^2 \bar{c} = 0. \tag{1.1}$$

Here c is the solute concentration, w is the longitudinal velocity, κ is the longitudinal molecular (or turbulent) diffusivity and D_0 is the shear dispersion coefficient. The overbars denote average values across the flow.

Even at high dilution it is difficult to avoid the effects of buoyancy. For horizontal flows Erdogan & Chatwin (1967) showed how to calculate the coefficient D_2 of the quadratic buoyancy correction $D_0 + D_2(\partial_z \bar{c})^2$ to the shear dispersion coefficient. The present paper deals with the somewhat simpler case of vertical flows. It is shown that the leading-order buoyancy correction takes the linear form $D_0 + D_1\,\partial_z \bar{c}$. The coefficient D_1 is calculated for a few flow geometries and a general formula is also derived. For z increasing upwards, the coefficient D_1 is positive if the solute increases the density.

In the context of flow in porous media Knight & Philip (1974) pointed out the desirability of exactly solvable nonlinear problems. They derived the two-parameter class of concentration-dependent diffusivities that can be solved by a linearizing transformation. The corresponding exactly solvable equation with gradient-dependent diffusion is

$$\partial_t \bar{c} + \bar{w}\,\partial_z \bar{c} - \partial_z\left(\frac{[\bar{\kappa}+D_0]}{1+\gamma\,\partial_z \bar{c}}\partial_z \bar{c}\right) = 0. \tag{1.2}$$

This is compatible with the leading-order buoyancy correction $D_0 + D_1\,\partial_z \bar{c}$ if the coefficients γ and D_1 are related:

$$\gamma = \frac{-D_1}{\bar{\kappa}+D_0}. \tag{1.3}$$

To test the range of accuracy of the model equation (1.2) an explicit solution is derived for the full nonlinear dependence $D(\partial_z \bar{c})$ of the shear dispersion coefficient for vertical plane Poiseuille flow. In the Appendix to this paper it is shown that when there is a strong unstable density gradient the flow becomes unstable (well before the approximate or exact expressions for $D(\partial_z \bar{c})$ exhibit any singularities). Nevertheless, prior to the instability the exactly solvable model gives reasonably accurate results for the buoyancy-modified shear dispersion coefficient.

2. Moving stretched coordinates

For simplicity we shall assume that the flow geometry is the same at all levels and that we can make the Boussinesq approximation (i.e. buoyancy effects are important but inertia changes are negligible). Thus, the cross-sectionally averaged longitudinal velocity $\bar{w}$ will be independent of longitudinal position z. (Buoyancy will affect the velocity profile but not the averaged flow.) We shall also assume that the flow can be modelled as if it were steady and laminar. The possibility of flow instability is addressed in the Appendix.

In the Taylor limit the mixing zone between the miscible Newtonian fluids has become greatly elongated and evolves very slowly as it is carried upwards at the mean velocity $\bar{w}$. To account explicitly for these features we introduce a small parameter ϵ which typifies the width-to-length aspect ratio of the mixing region. In terms of ϵ we replace the conventional longitudinal and time coordinates (z, t) by the moving stretched coordinates

$$\zeta = \epsilon(z - \bar{w}t), \quad \tau = \epsilon^2 t. \tag{2.1 a, b}$$

If the Cartesian velocity components for nearly longitudinal flow are $(\epsilon u, \epsilon v, w)$ then, with density changes neglected, the conservation of mass equation takes the form

$$\partial_x u + \partial_y v + \partial_\zeta w = 0. \tag{2.2}$$

The flow geometry will be characterized as being a zero contour of a function $\Omega(x, y)$. The condition for zero mass flux across the boundary is

$$u\,\partial_x \Omega + v\,\partial_y \Omega = 0 \quad \text{on} \quad \Omega = 0. \tag{2.3}$$

For a viscous fluid the velocity components u, v are separately zero on a stationary solid boundary.

The cross-sectional average of (2.2) gives the result

$$\partial_\zeta \bar{w} = 0. \tag{2.4}$$

as has been assumed already.

3. Taylor limit

For isotropic molecular diffusion the concentration fraction $c(x, y; \zeta, \tau)$ of one miscible fluid in the other satisfies the equation

$$\epsilon[\epsilon\,\partial_\tau c + u\,\partial_x c + v\,\partial_y c + (w-\bar{w})\,\partial_\zeta c] = \partial_x(\kappa\,\partial_x c) + \partial_y(\kappa\,\partial_y c) + \epsilon^2\,\partial_\zeta(\kappa\,\partial_\zeta c). \quad (3.1)$$

Since we are not restricting our attention to dilute concentrations, the diffusivity κ may be a function of the concentration c. Changes in the surrounding bed-rock temperature as the mixing zone rises might also give τ-dependence to κ. The condition for zero diffusive flux across the impermeable boundary is

$$\kappa\nabla_{\mathrm{H}} c\cdot\nabla_{\mathrm{H}}\Omega = 0 \quad \text{on} \quad \Omega = 0, \quad (3.2)$$

where ∇_{H} denotes the horizontal gradient operator (∂_x, ∂_y). The mass flux boundary condition (2.3) already ensures that there is zero advective flux of concentration across the boundary. For turbulent flows an eddy diffusivity would replace the molecular diffusivity.

At leading order in the small parameter ϵ the concentration becomes uniform across the flow:

$$c = \bar{c}(\zeta, \tau) - \epsilon f(x, y; \zeta, \tau)\,\partial_\zeta \bar{c} + \dots. \quad (3.3)$$

Thus, to a first approximation the concentration-dependent diffusivity κ is likewise constant across the flow. The function f is called the centroid displacement function and gives the relative longitudinal position of constant-concentration surfaces (i.e. the displacement from the centroid). The equations and boundary conditions satisfied by f are

$$\bar{\kappa}\nabla_{\mathrm{H}}^2 f = \bar{w} - w, \quad (3.4a)$$

with

$$\nabla_{\mathrm{H}} f\cdot\nabla_{\mathrm{H}}\Omega = 0 \quad \text{on} \quad \Omega = 0 \quad (3.4b)$$

and

$$\bar{f} = 0. \quad (3.4c)$$

Since the velocity profile w is buoyancy-modified and depends upon the concentration gradient $\partial_\zeta \bar{c}$, the same will be true of the centroid displacement function f.

If we average the concentration evolution equation (3.1) across the flow, then by virtue of the near uniformity of the concentration and the conservation of mass, we find that the order-1 and order-ϵ terms integrate to zero. The remaining order-ϵ^2 terms yield the Taylor shear dispersion equation

$$\partial_\tau \bar{c} - \partial_\zeta([\bar{\kappa} + D]\,\partial_\zeta \bar{c}) = 0, \quad (3.5a)$$

where

$$D = \overline{(w-\bar{w})f} = \bar{\kappa}\overline{(\nabla_{\mathrm{H}} f)^2}. \quad (3.5b)$$

Back in the original stationary z, t coordinates the evolution equation for $\bar{c}$ becomes

$$\partial_t \bar{c} + \bar{w}\,\partial_z \bar{c} - \partial_z([\bar{\kappa} + D(\partial_z \bar{c})]\,\partial_z \bar{c}) = 0. \quad (3.6)$$

Taylor (1953) was concerned with dilute solutes where the velocity profile w, centroid displacement f and shear dispersion coefficient D are unaffected by buoyancy. Here it is the buoyancy modifications that are of prime concern.

If we sought to replicate the work of Erdogan & Chatwin (1967), then we would have to allow all three velocity components (u, v, w) to be of the same order (i.e. strong gravitational forces across the principal flow direction gives rise to strong secondary flows). The equation (3.4a) for the centroid displacement function f would then have to include secondary flow advection terms $u\partial_x f + v\partial_y f$. Similar strong advection terms would complicate the calculation of the longitudinal velocity w as modified by buoyancy. Fortunately, the formula (3.5b) for the shear dispersion coefficient D remains valid.

If a is a representative transverse lengthscale for the flow, then we can deduce from (3.4a) that the centroid displacement function f scales as

$$f = \frac{\bar{w}a^2}{\bar{\kappa}} F(x, y; \zeta, \tau), \tag{3.7}$$

where F is a dimensionless function. Using this representation in (3.5b) we can replicate Taylor's (1953) celebrated scaling law for the shear dispersion coefficient:

$$D = \frac{\bar{w}^2 a^2}{\bar{\kappa}} d, \quad \text{with} \quad d = a^2 \overline{(\nabla_{\mathrm{H}} F)^2} \tag{3.8a,b}$$

where d is a dimensionless numerical factor.

4. Buoyancy-modified longitudinal velocity

For flows to which the Boussinesq approximation is applicable, the density ρ does not depart far from a reference density ρ_0. In the mixing zone the perturbation density $\epsilon^{\beta}\hat{\rho}$ will be a function of the concentration fraction c and may also vary with τ (via pressure or temperature changes):

$$\rho = \rho_0 + \epsilon^{\beta} \hat{\rho}(c, \tau). \tag{4.1}$$

The exponent β merely serves as a reminder that the density perturbation is small. The non-uniformity in concentration across the flow will give rise to a density non-uniformity:

$$\rho = \rho_0 + \epsilon^{\beta} \hat{\rho}(\bar{c}, \tau) - \epsilon^{1+\beta} + f(x, y; \zeta, \tau) \frac{\partial \hat{\rho}}{\partial c} \partial_{\zeta} \bar{c} + \ldots. \tag{4.2}$$

To a first approximation the pressure in the fluid mixture will be the (very large) hydrostatic pressure associated with the cross-sectionally averaged density $\rho_0 + \epsilon^{\beta}\hat{\rho}(\bar{c}, \tau)$. For the dynamic excess pressure $\epsilon^{-1}p$ and velocity components $(\epsilon u, \epsilon v, w)$ the dominant terms in the Navier–Stokes momentum equations are

$$\nabla_{\mathrm{H}} p = 0, \tag{4.3a}$$

$$\partial_{\zeta} p - g f \frac{\partial \hat{\rho}}{\partial c} \partial_{\zeta} \bar{c} = \bar{\mu} \nabla_{\mathrm{H}}^2 w, \tag{4.3b}$$

with $$w = 0 \quad \text{on} \quad \Omega = 0, \tag{4.3c}$$

and $$\bar{w} \text{ given.} \tag{4.3d}$$

Here $\epsilon^{-1-\beta}g$ is the downwards gravitational acceleration and $\bar{\mu} = \mu(\bar{c}, \tau)$ is the viscosity. The large weighting given to the excess pressure is a consequence of the large pressure drop needed to drive a flow over distances the size of the mixing region. The large weighting given to gravity is necessary if the buoyancy forces are to have a leading-order influence upon the longitudinal velocity profile. For turbulent flows an eddy viscosity would replace the laminar viscosity.

To quantify the magnitude of the buoyancy correction we introduce the dimensionless density gradient

$$G = \frac{a^4 g}{\bar{\mu}\bar{\kappa}} \frac{\partial \hat{\rho}}{\partial c} \partial_{\zeta} \bar{c} = -\frac{a^4 g}{\bar{\mu}\bar{\kappa}} \partial_{\zeta} \bar{\rho}. \tag{4.4}$$

G is positive when the density gradient is stable (i.e. decreasing upwards). The dimensionless counterpart to the coupled equations (4.3), (3.4) for w and f are

$$a^2\nabla^2_{\mathrm{H}} W = -P + GF, \tag{4.5a}$$

$$a^2\nabla^2_{\mathrm{H}} F = 1 - W, \tag{4.5b}$$

with

$$0 = W = \nabla_{\mathrm{H}} F \cdot \nabla_{\mathrm{H}} \Omega \quad \text{on} \quad \Omega = 0, \tag{4.5c}$$

$$\overline{W} = 1 \quad \text{and} \quad \overline{F} = 0. \tag{4.5d, e}$$

The dimensionless pressure gradient $P(G)$ is implicitly determined via the mass-flux constraint (4.5d) upon the buoyancy-modified velocity profile. A neat general result is

$$P = a^2\overline{(\nabla_{\mathrm{H}} W)^2} + Gd. \tag{4.6}$$

Even though we have already accounted for the hydrostatic pressure, we infer that the pressure gradient needed to drive the upwards flow is increased when there is a stable density gradient (G positive). A typical wavenumber across the flow would be π/a. So a value $G = \pi^4$ ($= 97.4$) would not be deemed large. Alas, the Appendix reveals that gravitation instability arises for the small value $G = -31$.

For Long's (1991) experiments the gap width $2a$ was 2.5 mm and the diffusivities for salt in water and for momentum had the approximate values

$$\bar{\kappa} \sim 10^{-3}\ \mathrm{mm^2\,s^{-1}}, \quad \bar{\mu}/\bar{\rho} \sim 1\ \mathrm{mm^2\,s^{-1}}. \tag{4.7}$$

For experiments with a density change of only one part per thousand over a vertical distance of 100 mm, the corresponding dimensionless density gradient is

$$G \sim 250. \tag{4.8}$$

Thus, the flow would be modified significantly by the effects of buoyancy. Long's (1991) experiments extended to density changes as large as 4% where the scalings used in the present paper are not pertinent. However, the Reynolds number of the flows ranged up to several thousand for which the flow would cease to be laminar. The much larger turbulent estimates for $\bar{\kappa}$ and $\bar{\mu}$ would greatly reduce the estimate of the dimensionless density gradient G down to values to which the present calculations are appropriate.

For oil wells the gap width could be a factor of ten larger, with G increased by a factor of 10^4. Thus, the present analysis would only be pertinent to turbulent flows. For example, with

$$2a = 25\ \mathrm{mm}, \quad \bar{w} = 100\ \mathrm{mm\,s^{-1}}, \quad \frac{\bar{\mu}}{\bar{\rho}} \sim \bar{\kappa} \sim 12.5\ \mathrm{mm^2\,s^{-1}} \tag{4.9}$$

and a change of density of 1% over a vertical distance of 10^3 mm, we obtain the estimate

$$G \sim 15. \tag{4.10}$$

Slower turbulent flows give smaller eddy viscosities and diffusitivies with larger values of the dimensionless density gradient.

5. Power series in buoyancy

For small dimensionless density gradient G (less than π^4) we can represent the velocity profile, pressure gradient and centroid displacement function as being small perturbations about non-buoyant flow:

$$W = W_0(x,y) + GW_1(x,y) + \ldots, \quad P = P_0 + GP_1 + \ldots, \quad F = F_0(x,y) + GF_1(x,y) + \ldots. \tag{5.1a, b}$$

The leading-order equations are

$$a^2\nabla_H^2 W_0 = -P_0, \tag{5.2a}$$

$$a^2\nabla_H^2 F_0 = 1 - W_0, \tag{5.2b}$$

$$0 = W_0 = \nabla_H F_0 \cdot \nabla_H \Omega \quad \text{on} \quad \Omega = 0, \tag{5.2c}$$

$$\overline{W_0} = 1, \quad \overline{F_0} = 0. \tag{5.2d, e}$$

The dimensionless leading-order shear dispersion coefficient d_0 has the positive value

$$d_0 = a^2\overline{(\nabla_H F_0)^2}. \tag{5.3}$$

The first-order correction terms satisfy the equations

$$a^2\nabla_H^2 W_1 = -P_1 + F_0, \tag{5.4a}$$

$$a^2\nabla_H^2 F_1 = -W_1, \tag{5.4b}$$

$$0 = W_1 = \nabla_H F_1 \cdot \nabla_H \Omega \quad \text{on} \quad \Omega = 0, \tag{5.4c}$$

$$0 = \overline{W_1} = \overline{F}_1. \tag{5.4d}$$

A simple consequence of these equations (or equivalently of the general result (4.6)) is that

$$P_1 = d_0. \tag{5.5}$$

The dimensionless first-order shear dispersion coefficient d_1 has the negative value

$$d_1 = 2a^2\overline{\nabla_H F_0 \cdot \nabla_H F_1} = -2a^2\overline{(\nabla_H W_1)^2}. \tag{5.6}$$

Hence, stable concentration gradients tend to decrease the longitudinal shear dispersion.

For plane Poiseuille flow between parallel plates $2a$ apart the leading-order solutions are

$$W_0 = \frac{3}{2}\left\{1 - \frac{y^2}{a^2}\right\}, \quad P_0 = 3, \tag{5.7a, b}$$

$$F_0 = \frac{1}{120}\left\{7 - 30\frac{y^2}{a^2} + 15\frac{y^4}{a^4}\right\}, \quad d_0 = \frac{2}{105}, \tag{5.7c, d}$$

where y is the distance from the mid-line. The first-order buoyancy corrections are

$$W_1 = \frac{1}{105}\left\{1 - \frac{y^2}{a^2}\right\} - \frac{1}{240}\left\{3 - 7\frac{y^2}{a^2} + 5\frac{y^4}{a^4} - \frac{y^6}{a^6}\right\}, \tag{5.8a}$$

$$F_1 = \frac{1}{105}\left\{\frac{9}{60} - \frac{y^2}{2a^2} + \frac{y^4}{12a^4}\right\} - \frac{1}{240}\left\{\frac{1021}{2520} - \frac{3y^2}{2a^2} + \frac{7y^4}{12a^4} - \frac{y^6}{6a^6} + \frac{y^8}{56a^8}\right\}, \tag{5.8b}$$

$$d_1 = -\frac{52}{363825}. \tag{5.8c}$$

At the centre of the flow ($y = 0$) the functions W_1 and F_1 are both negative. So stable density gradients (G positive) tend to flatten the velocity and centroid displacement profiles (i.e. the flow adjusts to reduce the amount of dense fluid conveyed a relatively long way upwards). We remark that plane Poiseuille flow is a good approximation to the majority of Long's (1991) experiments which involved narrow-gap flows between concentric cylinders.

In terms of the original (unscaled) z, t coordinates the two-term approximation for the shear dispersion coefficients is

$$D(\partial_z \bar{c}) = \frac{\bar{w}^2 a^2}{\bar{\kappa}}\left\{d_0 - d_1 \frac{a^4 g}{\bar{\mu}\bar{\kappa}}\frac{\partial \bar{\rho}}{\partial \bar{c}}\partial_z \bar{c} + \ldots\right\}, \tag{5.9c}$$

$$= D_0 + D_1 \partial_z \bar{c} + \ldots \tag{5.9b}$$

If the diffusivity $\bar{\kappa}$, viscosity $\bar{\mu}$ and the rate of density increase $\partial\bar{\rho}/\partial\bar{c}$ are independent of the concentration $\bar{c}$, then the coefficients D_0 and D_1 will likewise be independent of $\bar{c}$. If the density $\bar{\rho}$ increases with the solute concentration $\bar{c}$ then D_1 is positive (by virtue of d_1 being negative), i.e.

$$D_1 = -d_1 \bar{w}^2 \frac{a^6 g}{\bar{\mu}\bar{\kappa}^2}\frac{\partial \bar{\rho}}{\partial \bar{c}}. \tag{5.10}$$

For other flow geometries we can itemize the steps in the solution procedure:

(1) solve the Poisson equation (5.2 a) for the non-buoyant pressure gradient P_0 and velocity profile $W_0(x,y)$;

(ii) solve the Poisson equation (5.2b) for the non-buoyant centroid displacement function $F_0(x,y)$;

(ii) Perform the cross-sectional averaging (5.3) to evaluate the non-buoyant shear dispersion coefficient $d_0 = P_1$;

(iv) solve the Poisson equation (5.4a) for the buoyancy correction $W_1(x,y)$ to the velocity profile;

(v) perform the cross-sectional averaging (5.6) to evaluate the (negative) buoyancy correction d to the shear dispersion coefficient.

For laminar flow in a cylindrical vertical pipe these five steps give the results

(i) $$P_0 = 8, \quad W_0 = 2\left\{1 - \frac{r^2}{a^2}\right\},$$

(ii) $$F_0 = \frac{1}{4}\left\{2 - 6\frac{r^2}{a^2} + 3\frac{r^4}{a^4}\right\},$$

(iii) $$d_0 = P_1 = \tfrac{1}{48},$$

(iv) $$W_1 = \frac{1}{64}\left\{\frac{r^2}{a^2} - \frac{r^4}{a^4}\right\} - \frac{1}{288}\left\{1 - \frac{r^6}{a^6}\right\},$$

(v) $$d_1 = -(1 + \tfrac{1}{240})/576,$$

where r is the radial coordinate and a the pipe radius. The non-buoyant results (i)–(iii) replicate the well-known solutions given by Taylor (1953).

6. Exactly solvable nonlinear diffusion equation

If we replace the concentration $\bar{c}$ by the slope

$$s = \partial_z \bar{c} \tag{6.1}$$

as the dependent variable, then the nonlinear diffusion equation (3.6) for $\bar{c}(z,t)$ with gradient-dependent diffusivity $[\bar{\kappa} + D(\partial_z \bar{c})]$ is equivalent to the equation

$$\partial_t s + \bar{w}\,\partial_z s - \partial_z([\bar{\kappa} + D + s\,\partial_s D]\,\partial_z s) = 0, \tag{6.2}$$

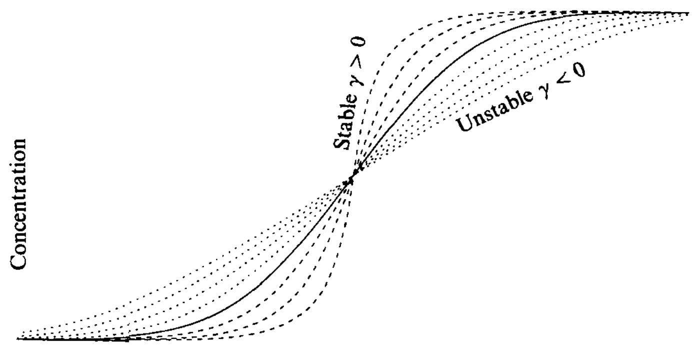

FIGURE 1. The effect of nonlinearity upon the shape of a concentration surge.

with s-dependent diffusivity. Knight & Philip (1974) showed that an exact linearizing transformation is possible if and only if (6.2) takes the form

$$\partial_t s + \bar{w}\,\partial_z s - \partial_z\left(\frac{[\bar{\kappa}+D_0]}{(1+\gamma s)^2}\partial_z s\right) = 0. \tag{6.3}$$

The combination $[\bar{\kappa}+D_0]$ is the limiting linear diffusivity and the parameter γ quantifies the nonlinearity. Thus, we can infer that the original equation (3.6) for $\bar{c}(z,t)$ has an exact linearizing transformation if and only if the gradient-dependent takes the form

$$\bar{\kappa}+D(\partial_z \bar{c}) = \frac{[\bar{\kappa}+D_0]}{1+\gamma\,\partial_z \bar{c}}. \tag{6.4}$$

As noted in the introduction, the two-term approximation (5.9*b*) for the gradient-dependent shear dispersion coefficient is compatible with the exactly solvable model provided that the parameter γ has the value

$$\gamma = \frac{-D_1}{\bar{\kappa}+D_0}. \tag{6.5}$$

In the usual limit, in which shear dispersion D_0 greatly dominates molecular diffusion $\bar{\kappa}$, we can evaluate γ:

$$\gamma = -\frac{d_1}{d_0}\frac{a^4 g}{\bar{\mu}\bar{\kappa}}\frac{\partial\rho}{\partial c}. \tag{6.6}$$

If the density increases with increasing concentration c, then γ is positive (because d_1 is negative).

For the exactly solvable nonlinear diffusion equation (1.2) the exact linearizing transformation merely involves a change of coordinate from z to

$$Z = z + \gamma\bar{c}(z,t). \tag{6.7}$$

In terms of the auxiliary coordinate Z the concentration $\bar{c}(Z,t)$ satisfies the linear diffusion equation (1.1). From a solution $\bar{c}(Z,t)$ of the linear equation (1.1) we can construct a solution $\bar{c}(z,t)$ of the nonlinear equation (1.2) merely by a coordinate distortion:

$$z = Z - \gamma\bar{c}(Z,t). \tag{6.8}$$

Figure 1 shows the relative shapes of concentration profiles for a range of γ-values.

A necessary condition for the forwards transformation (6.7) to be single valued is that

$$-1 < \gamma\,\partial_z \bar{c}, \tag{6.9a}$$

and for the backwards transformation (6.8) the corresponding constraint is

$$\gamma \partial_Z \bar{c} < 1. \tag{6.9b}$$

Outside this regime the model equation (1.2) is ill-posed and is violently unstable. The Appendix to this paper reveals that the flow has already become unstable before this condition (6.9*a*) is violated.

For the nonlinear diffusion equation (3.6) a small perturbation $\delta\bar{c}$ satisfies the linear equation (cf. (6.2))

$$\partial_t \delta\bar{c} + \bar{w}\, \partial_z \delta\bar{c} - \partial_z([\kappa + \partial_s(sD)]\, \partial_z \delta\bar{c}) = 0. \tag{6.10}$$

A necessary condition for well-posedness and stability is that $\bar{\kappa} + \partial_s(sD)$ be positive. It is this condition that is violated outside the region defined by the constraint (6.9*a*).

7. Buoyancy-modified vertical plane Poiseuille flow

For vertical laminar flow between parallel plates it is possible to derive an explicit solution for the dimensionless velocity profile $W(y/a\,;G)$ and hence the dimensionless shear dispersion coefficient $d(G)$.

If we eliminate the dimensionless centroid displacement function $F(y/a;\, G)$, then (4.5*a b*) can be combined to give a fourth-order linear ordinary differential equation for $W(y/a\,;G)$:

$$\frac{\mathrm{d}^4 W}{\mathrm{d}Y^4} + GW = G, \quad \text{with} \quad Y = y/a. \tag{7.1 a b}$$

In the unstable case (G negative) we define the real parameter

$$\Lambda = (-G)^{\frac{1}{4}}, \tag{7.2}$$

and we represent the symmetric velocity profile:

$$W = 1 - \frac{(\sin \Lambda \cosh \Lambda Y - \sinh \Lambda \cos \Lambda Y)}{(\sin \Lambda \cosh \Lambda - \sinh \Lambda \cos \Lambda)}. \tag{7.3}$$

In the stable case (G positive) we define the real parameter

$$l = (\tfrac{1}{4}G)^{\frac{1}{4}}, \tag{7.4}$$

and we represent the symmetric velocity profile:

$$W = 1 + \frac{(\cosh l \sin l - \sinh l \cos l) \cosh lY \cos lY - (\cosh l \sin l + \sinh l \cos l) \sinh lY \sin lY}{\cosh l \sinh l - \cos l \sin l}. \tag{7.5}$$

Figure 2(*a*) shows these velocity profiles for several values of G. In the unstable case there is flow reversal at

$$\Lambda = \pi, \quad \text{i.e.} \quad G = -\pi^4 = -97.4 \tag{7.6}$$

and a singularity when Λ reaches the first non-zero root of the transcendental equation

$$\tan \Lambda = \tanh \Lambda, \quad \text{i.e.} \quad \Lambda = 3.9266, \quad G = -237.7. \tag{7.7}$$

Figure 2(*b*) gives tests at the comparatively large values $G = -100$, 100 of the small-G approximation

$$W_0 + GW_1. \tag{7.8}$$

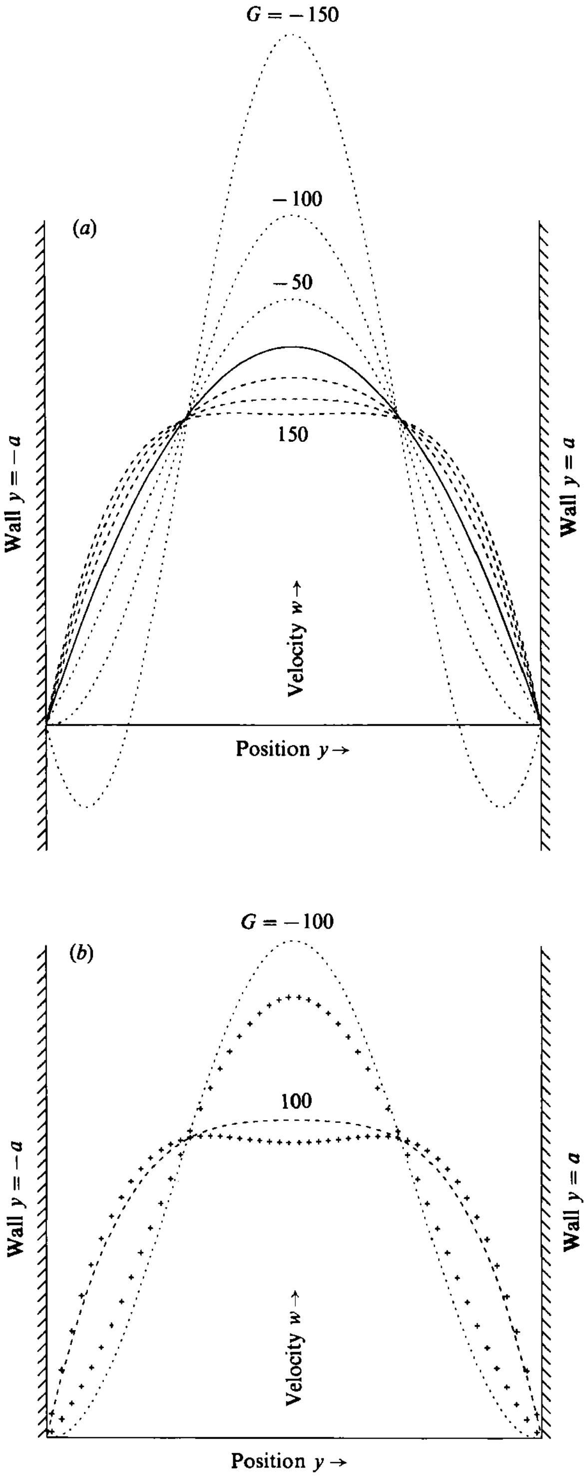

FIGURE 2. (*a*) The velocity profile for buoyancy-modified vertical plane Poiseuille flow. The parameter $G = -a^4 g\, \partial_z \rho / \kappa\mu$ is positive when the density gradient is stable. (*b*) Comparison between the exact and weak buoyancy approximations (+ + +) to the velocity profile for vertical plane Poiseuille flow with $G = -100, 100$.

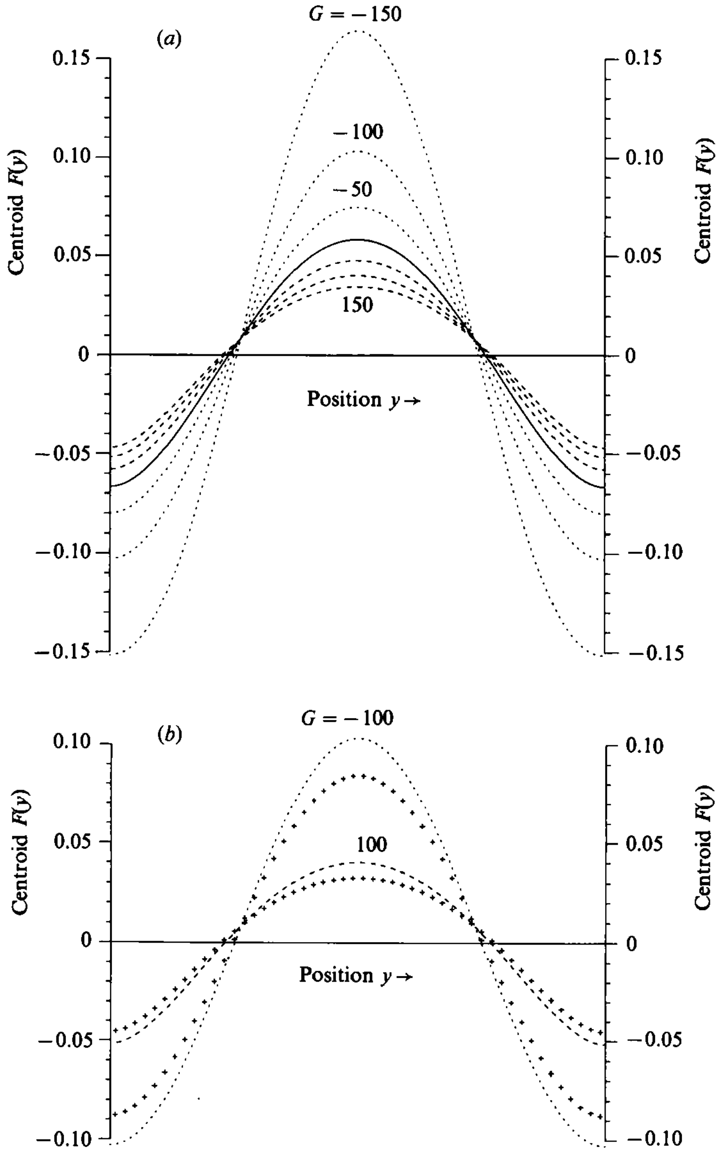

FIGURE 3. (*a*) The dimensionless centroid displacement function for buoyancy-modified vertical plane Poiseuille flow. (*b*) Comparison between the exact and weak buoyancy approximations ($+++$) to the centroid displacement function for vertical plane Poiseuille flow with $G = -100, 100$.

From the solutions (7.3), (7.5) for the dimensionless velocity profile, it is straightforward to solve (4.5*b*) for the dimensionless centroid displacement function:

$$F = \frac{\Lambda \sin\Lambda \cosh \Lambda Y + \Lambda \sinh \Lambda \cos \Lambda Y - 2\sin\Lambda \sinh\Lambda}{\Lambda^3(\sinh\Lambda\cosh\Lambda - \sinh\Lambda\cos\Lambda)}, \tag{7.9a}$$

$$F = \frac{(\sinh^2 l + \sin^2 l - \mu(\cosh l \sin l + \cos l \sinh l)\cosh lY \cos lY - l(\cosh l \sin l - \cos l \sinh l)\sinh lY \sin lY}{2l^3(\cosh l \sinh l - \cos l \sin l)}. \tag{7.9b}$$

Figure 3(*a*) shows the centroid displacement function for the same values of G used to illustrate the velocity profiles. There are the same general features of flattening

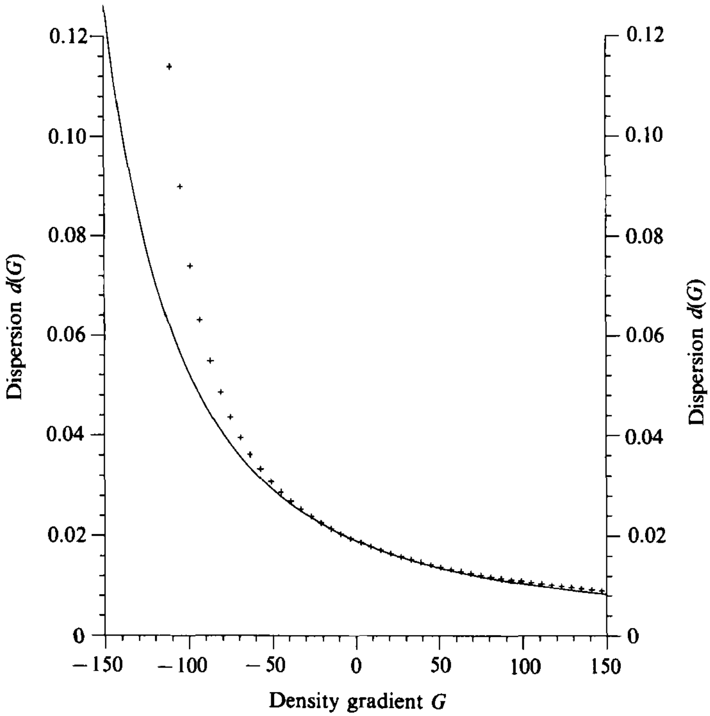

FIGURE 4. The shear dispersion coefficient for buoyancy modified vertical plane Poiseuille flow and the exactly solvable approximation (+ + +).

when the density gradient is stable and a sharpening for unstable density gradients. Figure 3(*b*) gives tests at $G = -100$, 100 of the small-G approximation

$$F_0 + GF_1. \tag{7.10}$$

To determine the dimensionless shear dispersion coefficient d we merely need to evaluate the integral (3.8*b*):

$$\mathrm{d} = \frac{2\Lambda\,(\cosh 2\Lambda + \cos 2\Lambda - 2) + (\cosh 2\Lambda - 1)\sin 2\Lambda - (1 - \cos 2\Lambda)\sinh 2\Lambda}{8\Lambda^3(\sin\Lambda\cosh\Lambda - \sinh\Lambda\cos\Lambda)^2}, \tag{7.11a}$$

$$d = \frac{\sinh 2l\cosh 2l + \sin 2l\cos 2l - \cosh 2l\sin 2l - \sinh 2l\cos 2l - 4l(1 - \cosh 2l\cos 2l)}{8l^3(\sinh 2l - \sin 2l)^2}. \tag{7.11b}$$

We remark that to the right of the singularity at $G = -237.7$ the flux $Gd(G)$ is an increasing function. Hence, away from the singularity the nonlinear shear dispersion equation is well-posed. However, the stability calculation given in the Appendix shows that the solution is physically relevant only for G greater than -31.

Figure 4 compares the exact results (7.11*a b*) with the simple approximation:

$$d = \frac{2}{105 + \frac{26}{33}G} \quad \text{for} \quad -133\tfrac{7}{26} < G. \tag{7.12}$$

For strongly unstable density gradients the approximation (7.12) wrongly predicts the position of the singularity and gives no indication of there being flow instability for G less than -31. However, the approximation is reasonably accurate for values of d ranging from half to one-and-a-half times the non-buoyant d_0.

I wish to thank Peter Long for his boundless enthusiasm and beautiful experiments. The need for the stability calculation was pointed out by the referees.

Appendix. Gravitational instability between parallel vertical plates

The calculations presented in the above paper cease to be valid if the flow is unstable. This Appendix investigates the stability of the particular case, studied in §7, of a Boussinesq fluid between parallel vertical plates. A simple instability criterion is derived for disturbances with long vertical lengthscale. The analysis is a miscible-fluid counterpart to long-wave instability calculations for immiscible fluids presented by Lister (1987) and by Smith (1989).

In the above paper it is assumed that the mixing zone is of great longitudinal extent. So, on a shorter lengthscale comparable with the plate separation $2a$, the unperturbed density distribution and flow can be represented:

$$\rho = \bar{\rho}(0)+z\frac{\mathrm{d}\bar{\rho}}{\mathrm{d}z}-\frac{a^2\bar{w}}{\bar{\kappa}}\frac{\mathrm{d}\bar{\rho}}{\mathrm{d}z}F(y)+\ldots, \quad w=\bar{w}W(y), \tag{A 1a, b}$$

As shown explicitly in §7, the y-dependence of the dimensionless centroid displacement function $F(y)$ and velocity profile $W(y)$ depend upon the local dimensionless density gradient

$$G=-\frac{a^4 g}{\bar{\mu}\bar{\kappa}}\partial_z\bar{\rho}. \tag{A 2}$$

If we now give a two-dimensional perturbation to this slowly varying flow, then the velocity perturbations v', w' can be represented in terms of a perturbation stream function ψ':

$$v'=-\partial_z\psi', \quad w'=\partial_y\psi'. \tag{A 3a, b}$$

The coupled equations satisfied by ψ' and the perturbation density ρ' are

$$\rho_0(\partial_t+\bar{w}(W-1)\,\partial_z)\,(\partial_y^2+\partial_z^2)\,\psi'-\rho_0\,\bar{w}\frac{\mathrm{d}^2W}{\mathrm{d}y^2}\partial_z\psi'-\bar{\mu}(\partial_y^2+\partial_z^2)^2\psi'=-g\,\partial_y\rho', \tag{A 4a}$$

$$(\partial_t+\bar{w}(W-1)\,\partial_z)\,\rho'-\bar{\kappa}(\partial_y^2+\partial_z^2)\,\rho'=-\frac{\mathrm{d}\bar{\rho}}{\mathrm{d}z}\partial_y\psi'+\frac{a^2\bar{w}}{\bar{\kappa}}\frac{\mathrm{d}\bar{\rho}}{\mathrm{d}z}\frac{dF}{dy}\partial_z\psi', \tag{A 4b}$$

with

$$\psi'=\partial_y\psi'=\partial_y\rho'=0 \quad \text{on} \quad y=\pm a. \tag{A 4c}$$

All quadratic and higher-order nonlinearities in the perturbation quantities ρ', ψ' have been ignored on the assumption that the perturbation is initially very small.

Since $\mathrm{d}\bar{\rho}/\mathrm{d}z$ varies slowly with respect to z and t, we can investigate the local stability of the perturbation ψ', ρ' as if all the coefficients in (A 4a, b) were independent of z and t. In particular, we can consider a single Fourier component

$$\psi'=\bar{\kappa}\Psi(y)\exp(\mathrm{i}\alpha z/a+\bar{\mu}\sigma t/\rho_0 a^2), \tag{A 5a}$$

$$\rho'=a\frac{\mathrm{d}\bar{\rho}}{\mathrm{d}z}\Phi(y)\exp(\mathrm{i}\alpha z/a+\bar{\mu}\sigma t/\rho_0 a^2), \tag{A 5b}$$

where

$$Y=y/a. \tag{A 5c}$$

Here Y is a dimensionless cross-stream coordinate, α is the dimensionless vertical wavenumber and σ is the dimensionless complex exponential growth rate. The coupled equations satisfied by the complex dimensionless functions $\Psi(Y)$, $\Phi(Y)$ are

$$(\sigma+\mathrm{i}Re\,\alpha(W-1))\left(\frac{\mathrm{d}^2}{\mathrm{d}Y^2}-\alpha^2\right)\Psi-\mathrm{i}Re\,\alpha\frac{\mathrm{d}^2W}{\mathrm{d}Y^2}\Psi-\left(\frac{\mathrm{d}^2}{\mathrm{d}Y^2}-\alpha^2\right)^2\Psi=G\frac{\mathrm{d}\Phi}{\mathrm{d}Y}, \quad \text{(A 6a)}$$

$$Pr(\sigma+\mathrm{i}Re\,\alpha(W-1))\,\Phi-\left(\frac{\mathrm{d}^2}{\mathrm{d}Y^2}-\alpha^2\right)\Phi=-\frac{\mathrm{d}\Psi}{\mathrm{d}Y}+\mathrm{i}Pr\,Re\,\alpha\frac{\mathrm{d}F}{\mathrm{d}Y}\Psi, \quad \text{(A 6b)}$$

with $\Psi=\frac{\mathrm{d}\Psi}{\mathrm{d}Y}=\frac{\mathrm{d}\Phi}{\mathrm{d}Y}=0$ on $Y=\pm 1$; where $Re=\frac{\bar{w}a\rho_0}{\bar{\mu}}$ and $Pr=\frac{\bar{\mu}}{\rho_0\bar{\kappa}}$ (A 6c–e)

Here Re is the Reynolds number and Pr is the Prandtl number. The condition for instability is that for some real value of the dimensionless vertical wavenumber α there is an eigenvalue σ for the time-dependence that has positive real part (exponential growth).

These formidable equations (A 6a–e) encompass the possibilities of instabilities associated with the density gradient $\mathrm{d}\bar{\rho}/\mathrm{d}z$, with the velocity profile $W(Y)$ or with both effects together (Drazin & Reid 1981, ch. 2, 4, 6). A limiting case in which the equations become tractable is when the vertical wavenumber α is zero:

$$\sigma\frac{\mathrm{d}^2\Psi}{\mathrm{d}Y^2}-\frac{\mathrm{d}^4\Psi}{\mathrm{d}Y^4}=G\frac{\mathrm{d}\Phi}{dY}, \quad Pr\,\sigma\Phi-\frac{\mathrm{d}^2\Phi}{\mathrm{d}Y^2}=-\frac{\mathrm{d}\Psi}{\mathrm{d}Y}. \quad \text{(A 7a, b)}$$

If we multiply (A 7a) by the complex conjugate Ψ^* of Ψ and we multiply the complex conjugate of (A 7b) by $G\Phi$, then by repeated integration by parts across the gap between the plates we can derive the identity

$$-\sigma\int_{-1}^{1}\left|\frac{\mathrm{d}\Psi}{\mathrm{d}Y}\right|^2\mathrm{d}Y-G\sigma^*Pr\int_{-1}^{1}|\Phi|^2\,\mathrm{d}Y=\int_{-1}^{1}\left|\frac{\mathrm{d}^2\Psi}{\mathrm{d}Y^2}\right|^2\mathrm{d}Y+G\int_{-1}^{1}\left|\frac{\mathrm{d}\Phi}{\mathrm{d}Y}\right|^2\mathrm{d}Y. \quad \text{(A 8)}$$

The individual integrands are all real and positive. For G positive we can deduce that the real part of σ is negative, i.e. that the perturbation is stable. Conversely, for G negative we can deduce that the imaginary part of σ is zero. So, as G decreases away from zero the transition between stability and instability occurs with $\sigma=0$.

For symmetric disturbances the eigenmodes for marginal stability ($\sigma=0$) have the explicit form

$$\Psi^{(0)}=\frac{\sinh\Lambda Y}{\sinh\Lambda}-\frac{\sin\Lambda Y}{\sin\Lambda}, \quad \Lambda\Phi^{(0)}=\frac{\cosh\Lambda Y}{\sinh\Lambda}+\frac{\cos\Lambda Y}{\sin\Lambda}, \quad \text{(A 9a, b)}$$

where $\tan\Lambda=\tanh\Lambda$ and $G^{(0)}=-\Lambda^4$. (A 9c, d)

The eigenvalue condition (A 9c) is precisely the singularity condition (7.7) encountered in the flow calculation. So the singularity in the nonlinear shear dispersion coefficient (7.11a) an be identified with the onset of symmetric instabilities.

For antisymmetric disturbances the eigenmodes for marginal stability ($\sigma=0$) have the representations

$$\Psi^{(0)}=\frac{\cosh\Lambda Y}{\cosh\Lambda}-\frac{\cos\Lambda Y}{\cos\Lambda}, \quad \Lambda\Phi^{(0)}=\frac{\sinh\Lambda Y}{\cosh\Lambda}-\frac{\sin\Lambda Y}{\cos\Lambda}, \quad \text{(A 10a, b)}$$

with $$\tanh \Lambda + \tan \Lambda = 0. \tag{A 10c}$$

The lowest non-trivial root for Λ is

$$\Lambda = 2.365, \quad \text{i.e.} \quad G^{(0)} = -31.28. \tag{A 11}$$

This antisymmetric instability (down at one side and up at the other) arises for a smaller density gradient $\mathrm{d}\bar{\rho}/\mathrm{d}z$ than that associated with symmetric disturbances. So, in practice the flows studied in this paper will have become unstable well before the singularity in the nonlinear shear dispersion coefficient can be approached. We remark that the instability criterion (A 11) coincides with the velocity profile (7.3) first having an inflexion point (at the boundaries).

In principle the circumstances in which the onset of instability is indeed associated with $\alpha = 0$ could be established by a long-wavelength solution confined to the marginal stability curve (with σ imaginary):

$$\sigma = \mathrm{i}\alpha\sigma^{(1)} + \mathrm{i}\alpha^3\sigma^{(3)} + \ldots, \quad G = -\Lambda^4 - \alpha^2 G^{(2)} - \alpha^4 G^{(4)} - \ldots, \tag{A 12a, b}$$

$$\Psi(Y;\alpha) = \Psi^{(0)}(Y) + \mathrm{i}\alpha\Psi^{(1)}(Y) + \alpha^2\Psi^{(2)}(Y) + \ldots, \tag{A 12c}$$

$$\Phi(Y;\alpha) = \Phi^{(0)}(Y) + \mathrm{i}\alpha\Phi^{(1)}(Y) + \alpha^2\Phi^{(2)}(Y) + \ldots, \tag{A 12d}$$

From (A 6*a*–*e*) it is easy to verify that the $\sigma^{(j)}$, $G^{(j)}$, $\Psi^{(j)}$ and $\Phi^{(j)}$ terms are all real. If the coefficient $G^{(2)}$ could be shown to be positive for the lowest antisymmetric mode, then it would follow that long waves are more unstable than short waves. Alas, the complexity of (A 6*a*–*e*) involving the velocity profile (7.3), the centroid displacement function (7.9*a*) as well as the eigenmodes (A 10*a*, *b*) has deterred the author from pursuing the general case.

A limiting case in which the above wavenumber expansion can be performed relatively easily is when there is a zero vertical mean flow. At order α^2 the stability equations (A 6*a*–*e*) yield the coupled equations

$$-\frac{\mathrm{d}^4\Psi^{(2)}}{\mathrm{d}Y^4} + \Lambda^4\frac{\mathrm{d}\Phi^{(2)}}{\mathrm{d}Y} = -2\Lambda^2\frac{\cosh\Lambda Y}{\cosh\Lambda} - 2\Lambda^2\frac{\cos\Lambda Y}{\cos\Lambda} + G^{(2)}\left(\frac{\cosh\Lambda Y}{\cosh\Lambda} - \frac{\cos\Lambda Y}{\cos\Lambda}\right), \tag{A 13a}$$

$$-\frac{\mathrm{d}^2\Phi^{(2)}}{\mathrm{d}Y^2} + \frac{\mathrm{d}\Psi^{(2)}}{\mathrm{d}Y} = \frac{\sinh\Lambda Y}{\Lambda\cosh\Lambda} - \frac{\sin\Lambda Y}{\Lambda\cos\Lambda}, \tag{A 13b}$$

with $$\Psi^{(2)} = \frac{\mathrm{d}\Psi^{(2)}}{\mathrm{d}Y} = \frac{\mathrm{d}\Phi^{(2)}}{\mathrm{d}Y} = \quad \text{on} \quad Y = \pm 1. \tag{A 13c}$$

If we multiply (A 13*a*) by $\Psi^{(0)}$ and (A 13*b*) by $\Lambda^4\Phi^{(0)}$, then by repeated integration by parts across the gap we can determine $G^{(2)}$:

$$G^{(2)}\int_{-1}^{1}\left(\frac{\cosh\Lambda Y}{\cosh\Lambda} - \frac{\cos\Lambda Y}{\cos\Lambda}\right)^2 \mathrm{d}Y = 2\Lambda^2\int_{-1}^{1}\left(\frac{\sinh\Lambda Y}{\cosh\Lambda} + \frac{\sin\Lambda Y}{\cos\Lambda}\right)^2 \mathrm{d}Y + \Lambda^2\int_{-1}^{1}\left(\frac{\sinh\Lambda Y}{\cos\Lambda} - \frac{\sin\Lambda Y}{\cos\Lambda}\right)^2 \mathrm{d}Y. \tag{A 14}$$

Since the integrands in (A 14) are all positive it follows that $G^{(2)}$ is positive. So, in this limiting case of zero vertical mean flow the gravitational instability is indeed associated with disturbances of long wavelength.

REFERENCES

DRAZIN, P. G. & REID, W. H. 1981 *Hydrodynamic Stability*. Cambridge University Press.

ERDOGAN, M. E. & CHATWIN, P. C. 1967 The effects of curvature and buoyancy on the laminar dispersion of solute in a horizontal tube. *J. Fluid Mech.* **29**, 465–484.

KNIGHT, J. H. & PHILIP, J. R. 1974 Exact solutions in nonlinear diffusion. *J. Engng Maths* **8**, 219–227.

LISTER, J. R. 1987 Long-wavelength instability of a line plume. *J. Fluid Mech.* **175**, 413–428.

LONG, P. J. G. 1991 Experimental studies of fluid–fluid displacement in annuli. Ph.D Thesis, Cambridge University.

SMITH, M. K. 1989 The axisymmetric long-wave instability of a concentric two-phase pipeflow. *Phys. Fluids* A **1**, 494–506.

TAYLOR, G. I. 1953 Dispersion of soluble matter in solvent flowing through a tube. *Proc. R. Soc. Lond.* A **216**, 186–203